

Robustness and Epistasis in the *C. elegans* Vulval Signaling Network Revealed by Pathway Dosage Modulation

Michalis Barkoulas,^{1,2,3} Jeroen S. van Zon,^{4,5} Josselin Milloz,^{2,6} Alexander van Oudenaarden,⁴ and Marie-Anne Félix^{1,2,3,*}

¹Institute of Biology of the Ecole Normale Supérieure

²Centre National de la Recherche Scientifique, UMR 8197

³Institut National de la Santé et de la Recherche Médicale U1024

46 rue d'Ulm, 75230 Paris Cedex 05, France

⁴Department of Biology, Massachusetts Institute of Technology (MIT), 77 Massachusetts Avenue, Cambridge, MA 02139, USA

⁵Present address: FOM Institute AMOLF, Science Park 104, 1098 XG Amsterdam, The Netherlands

⁶Present address: FAS Center for Systems Biology, Harvard University, 52 Oxford Street, Cambridge, MA 02138, USA

*Correspondence: felix@biologie.ens.fr

<http://dx.doi.org/10.1016/j.devcel.2012.12.001>

SUMMARY

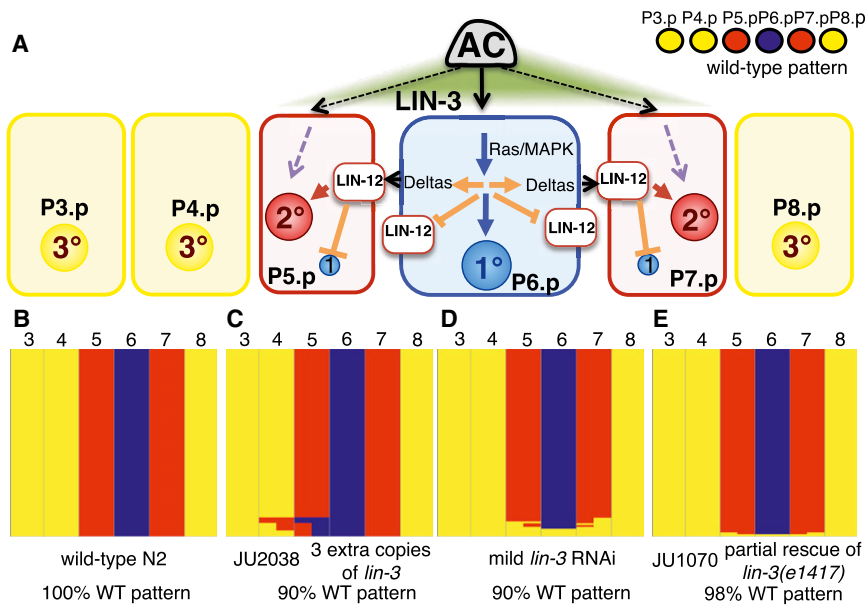
Biological systems may perform reproducibly to generate invariant outcomes, despite external or internal noise. One example is the *C. elegans* vulva, in which the final cell fate pattern is remarkably robust. Although this system has been extensively studied and the molecular network underlying cell fate specification is well understood, very little is known in quantitative terms. Here, through pathway dosage modulation and single molecule fluorescence in situ hybridization, we show that the system can tolerate a 4-fold variation in genetic dose of the upstream signaling molecule LIN-3/epidermal growth factor (EGF) without phenotypic change in cell fate pattern. Furthermore, through tissue-specific dosage perturbations of the EGF and Notch pathways, we determine the first-appearing patterning errors. Finally, by combining different doses of both pathways, we explore how quantitative pathway interactions influence system behavior. Our results highlight the feasibility and significance of launching experimental studies of robustness and quantitative network analysis in genetically tractable, multicellular eukaryotes.

INTRODUCTION

Developmental patterning systems can operate with astonishing precision and reproducibility akin to optimally engineered machines (Csete and Doyle, 2002). The property of a system to produce a relatively invariant output in the face of considerable variation, be it genetic, stochastic, or environmental, is called robustness (Wagner, 2005). The study of robustness has increasingly attracted the attention of biologists, because of its importance in understanding system behavior and evolution, but also due to its plausible implications in human disease (Kitano, 2004, 2007; Masel and Siegal, 2009). Although recent years

have seen an increase in theoretical studies addressing questions on robustness (Barkai and Leibler, 1997; von Dassow et al., 2000; Meir et al., 2002; Siegal and Bergman, 2002; Ma et al., 2006; Hoyos et al., 2011), experimental studies have remained very scarce, especially in multicellular eukaryotes (Eldar et al., 2002; Moriya et al., 2006; Gregor et al., 2007; Ansel et al., 2008; Braendle and Félix, 2008; Levy and Siegal, 2008). This is partly because of technical challenges in addressing the extent, limits, and mechanisms of robustness. A key challenge is to devise methods to precisely perturb a given system and then quantify the perturbations together with their phenotypic effects for the system (Masel and Siegal, 2009). To this end, the *Caenorhabditis elegans* vulva offers an excellent opportunity, as it is highly robust (Félix and Barkoulas, 2012) and readily amenable to genetic experiments, including transgenic manipulations. More importantly, both controlled dosage manipulations and quantitative techniques with single cell resolution have lately become available in *C. elegans* (Frøkjær-Jensen et al., 2008; Raj et al., 2008), paving the way for quantitative, perturbation-driven studies of robustness.

The *C. elegans* vulva has become a “textbook” example of intercellular communication driving animal organogenesis (Sternberg, 2005). Functionally, it is the egg-laying and copulatory organ of the adult hermaphrodite that is specified during the third larval stage (L3) of postembryonic development from a row of six epidermal precursor cells (Pn.p cells, numbered from P3.p to P8.p). Although these six Pn.p cells are all competent to adopt vulval fates, only three, P5.p–P7.p, are induced to form the vulva, whereas the other three (P3.p, P4.p, and P8.p) contribute to vulval tissues in situations when P5.p–P7.p fail to do so. Vulval induction involves two major signaling pathways, namely epidermal growth factor (EGF)-Ras-mitogen-activated protein kinase (MAPK) and Notch, which act together to specify three distinct cell fates (Sternberg and Horvitz, 1989; Sternberg, 2005) (Figure 1A). The master upstream inducer of vulval cell fates is LIN-3, a molecule similar to EGF (used here interchangeably with LIN-3), which is secreted by the anchor cell (Hill and Sternberg, 1992). As a consequence of LIN-3 secretion, the Ras-MAPK pathway is activated in P6.p, leading to the acquisition of the 1° cell fate (depicted throughout this paper in blue) and to the concomitant production of the Notch ligands (Figure 1A).



Subsequently, the 2° fate (depicted in red) is acquired by the neighboring P5.p and P7.p through paracrine Notch lateral signaling (Simske and Kim, 1995; Chen and Greenwald, 2004) (Figure 1A). LIN-3 may also act as a short-scale morphogen and directly promote, at low-dose, the 2° fate in P5.p and P7.p (Zand et al., 2011). The remaining cells of the competence group acquire the default 3° fate (depicted in yellow), and their daughters fuse with the hypodermis after one division (in about 50% of the individuals, P3.p fuses to the hypodermis without dividing). Therefore, the overall phenotypic space of this system is that of six competent cells acquiring one of three possible cell fates (Figure 1A).

Extensive genetic analysis over the last thirty years has yielded a good understanding of the molecular signaling network underlying vulval development. Nonetheless, even in such a well-studied system, systematic quantitative studies have been very limited, and very little is understood in quantitative terms (Katz et al., 1995). For example, we do know that *lin-3* expression is of paramount importance to vulval induction, as reduction of *lin-3* levels results in hypoinduced vulval phenotypes (where the average number of induced cells, also called induction index, is less than three), whereas *lin-3* overexpression leads to hyperinduction phenotypes (more than three cells induced). We also know that the system can tolerate some variation in *lin-3* expression, given that heterozygous animals for a null mutation in *lin-3* show a wild-type vulva cell fate pattern—that is, *lin-3* null mutations are recessive (Ferguson and Horvitz, 1985). However, a basic question concerning the EGF pathway remains unexplored: what is the *lin-3* dose range that allows the formation of a correct wild-type cell fate pattern?

A second basic question concerns the role of the Notch pathway in the vulval cell fate patterning network. LIN-12/Notch is thought to be playing a dual role in the vulval precursor cells, which is both to promote the 2° fate, but also to inhibit the 1° fate in P5.p and P7.p (Kenyon, 1995) (Figure 1A). Primary fate inhibition is implied by the *lin-12* loss-of-function mutant pheno-

type with adjacent 1° fates and mediated by direct targets inhibiting the phosphorylation of MAPK, such as the phosphatase *lip-1* (Berset et al., 2001; Yoo et al., 2004). Secondary fate promotion is supported by the excess of 2° fates in strong gain-of-function *lin-12* mutants (Greenwald et al., 1983). Although both LIN-12 functions are likely to be relevant for vulva development, it has remained difficult to disentangle which one, if any, prevails. This is mostly because LIN-12 is involved in anchor cell specification and can thus indirectly influence EGF signaling by altering the number of anchor cells in the somatic gonad. For example, strong *lin-12* loss-of-function mutants display two to four anchor cells (Greenwald et al., 1983; Sternberg and Horvitz, 1989) and thus show increased EGF signaling, whereas even weak *lin-12* mutations increase anchor cell number at a low penetrance and potentially *lin-3* expression (Sundaram and Greenwald, 1993). The effect of altering the Notch pathway specifically in the Pn.p cells thus remains unclear.

A third general question concerns the effects of variation in two components of a network. Extensive epistatic analysis has been performed in the vulva system, as in several other systems, by developmental geneticists seeking the relative position of genes in genetic pathways (Ferguson et al., 1987; Sternberg and Han, 1998; Sternberg, 2005). This type of epistasis analysis aims at defining upstream and downstream components in a given pathway and therefore requires null alleles to fully eliminate the activity of a gene product. On the other side, quantitative and population genetic theory ignores molecular pathways, but includes allelic variation at different loci. In this evolutionary framework, epistasis or gene interactions correspond to the nonadditive effect of combinations of alleles at two loci in a population (Phillips, 2008). Synthesizing laboratory and evolutionary genetics, it is becoming clear that quantitative variation in molecular pathways is central in accounting for phenotypic variation among individuals, be it stochastic, environmental, or genetic. Combinations of partial loss or gain-of-activity in molecular pathways within a network can inform on quantitative states of the

network (Gutiérrez, 2009; Corson and Siggia, 2012). Systematic combinations of alleles of different strengths have never been attempted, yet we argue that they are essential for a quantitative understanding of a system and its variational characteristics.

Here we thus sought out to investigate quantitative aspects of vulval development by experimentally perturbing the activity of the two main pathways involved in vulval patterning. First, we establish a LIN-3/EGF dose-response curve by performing dosage perturbations and then quantifying the degree of perturbation and the resulting phenotypic cell fate pattern for P3.p–P8.p. These experiments allow us to quantitatively define robustness by characterizing the range of *lin-3* dose variation compatible with the correct cell fate pattern. Second, by performing tissue-specific perturbations for the Notch pathway, we identify the first-appearing patterning errors to changes of its dose and contrast our tissue-specific LIN-12 downregulation to the existing results using *lin-12* mutants. Third, we combine dosage perturbations of the two pathways and investigate how the patterning system behaves. We uncover both synthetic interactions and unexpected, nonmonotonous system behavior. Our approach highlights emerging opportunities for experimental, quantitative studies of developmental robustness and network behavior in model eukaryotes.

RESULTS

Robustness and First-Appearing Errors to EGF Dose Variation

We started our experimental perturbations with the major pathway involved in vulval induction, the LIN-3/EGF pathway. To vary LIN-3 dose, we used a combination of transgenic manipulations, a cis-regulatory mutation, and RNA interference (RNAi). First, to increase the *lin-3* dose compared to the reference strain N2, we created lines with additional copies of *lin-3* at defined chromosomal positions, using the *Mos1*-mediated single copy insertion (MosSCI) methodology (Frøkjær-Jensen et al., 2008). We observed that the addition of three extra copies of *lin-3* per haploid genome, as in strain JU2038 (Figures 1B and 1C), was necessary to disturb the normal vulval cell fate pattern and led to about 10% penetrant errors, whereas no defects were found in animals carrying either one or two additional copies of *lin-3* (Figures S1A–S1C available online). We determined that the nature of the errors in JU2038 was mostly induction of P4.p, while P5.p acquired a half or full 1° fate (Figures 1C and S1A).

To support this finding and obtain more perturbation lines, we produced integrated multicopy transgenes, expressing different levels of *lin-3*, by introducing a genomic *lin-3* fragment under its anchor cell specific enhancer (Hwang and Sternberg, 2004). To obtain lines that represent the first errors to increasing LIN-3 dose, we created arrays with few *lin-3* copies by diluting the *lin-3* transgene with carrier DNA in the injection mix. We were able to recover both phenotypically silent lines for the vulva (that is, aphenotypic lines with induction index of 3), but also lines with induction index higher than 3, such as JU1105, which largely phenocopies JU2038 (Figure S1A).

To decrease LIN-3 dose, we used *lin-3* RNAi treatment by feeding the worms with *E. coli* bacteria, producing double-stranded RNAs corresponding to a *lin-3* fragment. Such a treatment in the N2 reference strain phenocopies strong loss-

of-function mutations in *lin-3* (Figure S1A). To define the first errors upon downregulation of *lin-3*, we diluted the double-stranded RNA-producing bacteria with control bacteria to reach concentrations that gave rise to low-penetrance errors, whereas a treatment with even higher dilutions did not alter the cell fate pattern (Figures 1D and S1A). We observed that the first errors upon *lin-3* downregulation were either loss of 2° fate for P5.p and P7.p or loss of all induced fates (Figure 1D). We were unable to uncouple these two phenotypes, depending on the dose of the RNAi treatment, indicating that the transition from wild-type pattern to loss of all induced fates is very steep.

To further support this result, we decreased *lin-3* dose to levels lower than N2 by overexpressing a *lin-3* genomic fragment containing the *lin-3(e1417)* promoter mutation that substantially diminishes *lin-3* expression (Hwang and Sternberg, 2004) into the *lin-3(e1417)* mutant background. We recovered rescued aphenotypic lines with induction index of 3 ($n > 100$), but also one line, JU1070 (Figure 1E), which showed concurrent loss of 2° fates and complete loss of induction, both at low penetrance, thus supporting the RNAi results.

Taken together, using the above approaches, we obtained a series of lines that displace the vulval induction index toward the hypoinduced or hyperinduced side. Notably, the relationship between variance and mean induction index is nonmonotonous, with low variance at vulval induction indices of 0, 3, and 6 and two peaks of high variance in between (Figure S1D). This pattern of variance denotes the intrinsic robustness of the wild-type system around index 3, where variance is zero. Perturbations that shift the mean induction index also increase its variance (Figure S1D), as they result in partial penetrant changes of induction for P5.p–P7.p at low *egf* doses and for P3.p, P4.p, and P8.p at high doses. At the two extremes, i.e., in the absence of any inductive signal or when the signal reaching the Pn.p cells is saturated, none, or all six, competent cells acquire vulval fates respectively, so variance is again zero.

Quantification of *lin-3* Expression in the Anchor Cell

To determine the range of *lin-3* dose variation to which the system is robust, we sought to quantify the level of *lin-3* expression in the perturbation lines, using a quantitative technique with single cell resolution, single molecule fluorescence in situ hybridization (smFISH) (Raj et al., 2008, 2010). This technique has been successfully used in *C. elegans*, for transcripts including *lin-3* (Saffer et al., 2011), to localize single messenger RNA (mRNA) molecules as quantifiable, diffraction-limited fluorescent spots.

We quantified *lin-3* mRNA number during the L3 stage for all EGF perturbation lines in synchronized populations (Figures 2A, 2B, and S2A–S2D). EGF perturbations are expected to alter *lin-3* expression specifically in the anchor cell; thus, we used *lag-2* as a marker to delimit the position and boundaries of this cell (Figure 2A). *lag-2* is also expressed in the distal tip cells of the gonad (Figure S2D) and in P6.p when induction has occurred (Figure 2A). Distal tip cell expression of *lag-2* was useful to estimate gonad length as a proxy for developmental stage and thus control for variation in growth of individual worms within synchronized populations.

In the N2 reference strain, the number of mRNAs first slightly increases during development, but soon becomes fairly steady (Figure S2B for gonad length 44–163 μm , mean = 26.6 ± 1.1

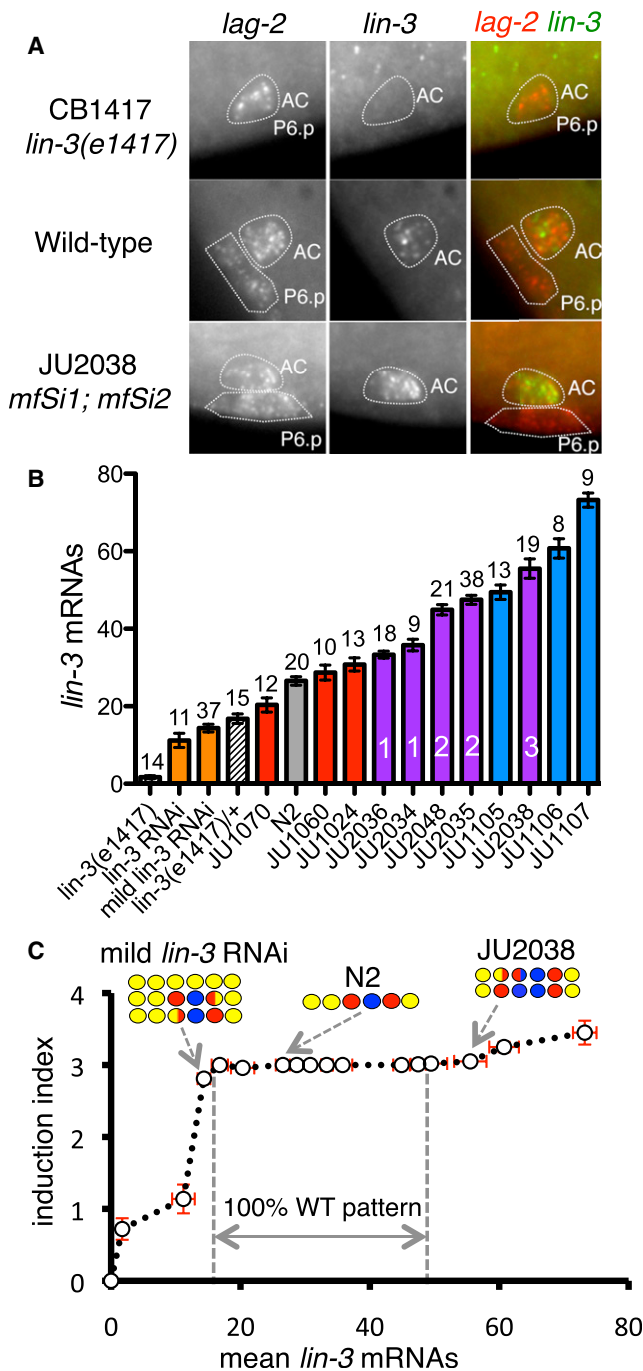


Figure 2. Quantification of *lin-3* Expression in the Perturbation Lines
 (A) Detection of *lag-2* and *lin-3* by smFISH in L3 larvae of CB1417 (*lin-3(e1417)*), N2, and JU2038 (*mfSi1; mfSi2*) strains. Left panels show *lag-2* signal, middle panels *lin-3*, and right panels an overlay of both signals (*lag-2* is in red and *lin-3* in green).

(B) Quantification of the mean number of *lin-3* mRNAs detected by smFISH in all perturbation lines. Bars are color-coded to indicate the nature of the perturbation: orange bars indicate RNAi experiments, red bars are used for lines obtained by injecting the *lin-3(e1417)* sequence into the *lin-3(e1417)* mutant, blue bars for lines obtained by injections of wild-type *lin-3* into N2, purple bars for *lin-3* MosSCI lines, where the number of insertions per haploid genome is presented within the bar, the gray bar for N2, and dashed bars for *lin-3(e1417)* homozygous or heterozygous animals. Error bars represent

standard error, range ≈ 17 –34 molecules, $n = 20$). Therefore, we used this time window for our quantifications, which corresponds to the time of induction of Pn.p cells until the first Pn.p cell division. The average number of mRNAs was the lowest in the *lin-3(e1417)* mutant (mean = 1.7 ± 0.4 mRNA molecules) and reached the highest measurable values in lines that overexpress multiple copies of *lin-3*, such as JU1107 (mean = 73.2 ± 1.82 mRNAs) (Figure 2B). We ordered the lines from lowest to highest mean mRNA number, which largely correlated with the phenotypic induction index ranking (Figures 2B and S2C).

Quantification of *lin-3* mRNAs in lines with the first errors upon EGF dose variation was particularly important to define the range of variation in *lin-3* expression that the system can buffer. For the hyperinduction robustness boundary, line JU2038 (induction index 3.07) was found to present an average mRNA number of 55.7 ± 2.5 and line JU1105 (induction index 3.025) an average of 49.5 ± 1.8 molecules. We observed that addition of increasingly more *lin-3* MosSCI copies increased linearly the number of mRNA molecules, although each copy added fewer mRNAs than the wild-type *lin-3*, perhaps due to the fact that our *lin-3* fragment does not reconstitute the full *lin-3* genomic locus (Figure S2E). Moreover, in keeping with the adjacent 1° fate phenotype in lines such as JU2038, we observed some P5.p cells expressing *lag-2*, while *lag-2* expression is strictly confined to P6.p in the N2 context (Figure S2F). For the hypoinduction boundary, *lin-3(e1417)* heterozygous animals that are completely aphenotypic for the vulva show 16.8 ± 1.26 *lin-3* mRNAs (range 11–25) on average, whereas dilutions of *lin-3* RNAi that show the first patterning errors were found to display an average of 14.4 ± 1 *lin-3* mRNA molecules (range 5–27 molecules). Taken together, we conclude that the vulva system is robust to genetic variation in *lin-3* expression between an average expression level of 15 and 50 *lin-3* mRNAs. Any variation in *lin-3* dose within these boundary values is predicted to be phenotypically silent for vulval patterning (Figure 2C). However, it is important to clarify that what we measured here is a correlation between mean *lin-3* mRNAs in the anchor cell and patterning errors in the Pn.p cells and not a correlation between *lin-3* expression and cell fate in individual animals. Since the first deviant patterns occur at low penetrance, it is possible that these errors are associated with some extreme values of the respective *lin-3* mRNA distributions (Figure S2C, compare minimum values of distribution between mild *lin-3* RNAi or JU1070, which both show vulval errors, to *lin-3(e1417)* heterozygotes, which do not).

First Errors to Tissue-Specific Notch Dosage Perturbations

The second key signaling pathway involved in vulval cell fate patterning is the LIN-12/Notch pathway, which is activated downstream of the EGF pathway through the transcriptional

standard error of the mean and numbers above each bar the number of animals analyzed.

(C) Graph showing the vulval induction index for each perturbation line as a function of the number of detected *lin-3* mRNAs. The robustness range to *lin-3* genetic dose variation is the area between the first errors on both sides of the wild-type N2 dose. X error bars represent standard error of the mean mRNA number and Y error bars standard error of the mean induction index. See also Figure S2.

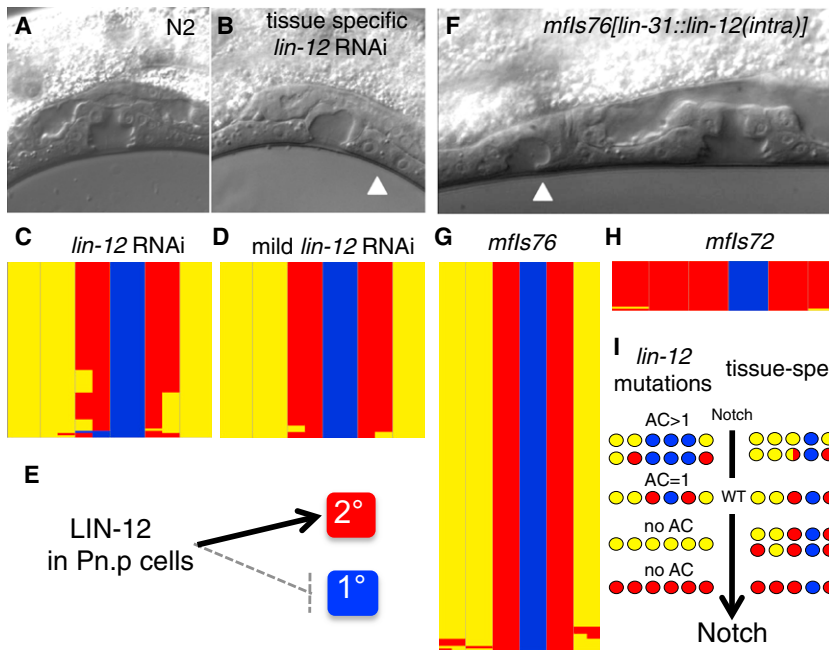


Figure 3. Tissue-Specific Notch Perturbations Define the First Patterning Errors

(A and B) Nomarski pictures of the L4 stage vulva in wild-type (A) and *lin-12* RNAi-treated animals carrying a *lin-31::rde-1* transgene in a *rde-1* mutant background (JU2039) (B). Arrowhead in (B) marks a P7.p cell that has not been induced, whereas P5.p is half induced.

(C and D) Phenotypic scoring of P3.p–P8.p fates in a representative Pn.p-specific *lin-12* RNAi experiments, with no dilution of the RNAi expression bacteria ($n = 79$) (C) or 3-fold dilution with control bacteria ($n = 83$) (D). We never observed similar defective vulval lineages in animals grown on control, vector-only, bacteria ($n > 500$).

(E) Cartoon depicting the prevailing function of Notch within Pn.p cells to promote the 2° fate, rather than inhibit the 1° fate.

(F) Nomarski picture of the L4 stage vulva in JU2064 (*mfls76[lin-31::lin-12(intra)]*); arrowhead marks an ectopic 2° fate induction.

(G and H) Phenotypic scoring in two lines with different levels of activated *lin-12/Notch* expression: JU2064 (*mfls76[lin-31::lin-12(intra)]*), $n = 162$ (G) and JU2060 *mfls72[lin-31::lin-12(intra)]*, $n = 26$ (H).

(I) Cartoon summarizing the cell fate patterns observed when increasing or decreasing Notch signaling in the Pn.p cells and their comparison to *lin-12* weak loss-of-function and gain-of-function mutants. WT stands for wild-type N2 pattern.

See also Figure S3 and Table S1.

upregulation of Deltas (Chen and Greenwald, 2004). Similar to the EGF pathway perturbations, we wanted to identify the first deviant patterns upon Notch pathway activity variation, specifically within the Pn.p cells, without affecting anchor cell determination. To vary Notch pathway dose, we decided to tune the expression of the Notch receptor LIN-12, as we found that overexpression of Deltas from their endogenous regulatory sequences does not perturb wild-type vulval cell fate patterning.

To decrease Notch dose in a tissue-specific way, we developed a strain for vulval precursor cell-specific RNAi. This method is based on tissue-specific rescue of the RNAi-deficient *rde-1* mutant of *C. elegans* (Qadota et al., 2007). We used the *lin-31* promoter, which is specifically expressed in the vulval precursor cells (Tan et al., 1998), to drive expression of the wild-type *rde-1(+)* sequence. RNAi then should function exclusively in the Pn.p cells. Indeed, by introducing *let-858::GFP* and *cdh-3::GFP* reporters and performing GFP RNAi, we verified that, in the tissue-specific RNAi background, gene expression is downregulated only in the Pn.p cells, but not in other tissues, such as the anchor cell or the seam cells (Figures S3A–S3D; Table S1). The available bacterial clone for *lin-12* RNAi by feeding in *C. elegans* worked poorly in our hands, so we produced a more efficient clone that can be used to phenocopy the extra-anchor-cell phenotype of *lin-12* mutants when used non-tissue-specifically (Figures S3E and S3F). When we then knocked down *lin-12* expression, specifically in the vulval precursor cells, we observed mainly a loss of 2° fates for P5.p and P7.p (Figures 3A–3C). By diluting the RNAi bacteria with control bacteria, we showed that this phenotype represents the first-appearing error upon decrease in Notch dose (Figure 3D). Thus, the phenotype we observed for tissue-specific *lin-12* downregulation suggested that the promotion of 2° fates is the most impor-

tant role of the Notch pathway for Pn.p cell patterning, rather than the inhibition of 1° fate, at least in the N2 background and in standard culture conditions (Figure 3E).

To further test this idea, we compared the results of tissue-specific *lin-12* RNAi with RNAi performed in a non-tissue-specific way in N2 (Figures 4A–4E). Similar to the tissue-specific phenotypes, and in contrast to the *lin-12* loss-of-function mutants, *lin-12* downregulation mostly led to loss of 2° fates in N2 (Figure 4A). We wondered whether this result reflects poor downregulation of *lin-12*, so we used an *rff-3* mutation to increase the sensitivity to RNAi (Simmer et al., 2002). Notably, when we performed *lin-12* RNAi at the whole animal level in the *rff-3(pk1426)* background, we observed that the most frequent phenotype was adjacent 1° fates for P5.p and P6.p (Figure 4B). However, this increased frequency of the adjacent 1° fate phenotype was not observed when the same *rff-3* mutation was introduced into the tissue-specific RNAi strain (Figures 4C–4E). Given that some animals with adjacent 1° fates can always be observed upon tissue-specific *lin-12* downregulation, the inhibitory role of LIN-12 on 1° fate cannot be merely associated with a change in anchor cell number. We conclude that the major role of LIN-12 in the Pn.p cells is to promote the 2° fate and, to a lesser extent, to inhibit the 1° fate (Figure 3E).

To increase Notch pathway activity in the Pn.p cells, we expressed a stabilized form of the active intracellular Notch domain under the Pn.p cell-specific promoter *lin-31* (Struhl et al., 1993; Tan et al., 1998). To obtain lines with a wide spectrum of penetrance of vulval defects, we used different dilutions of the injection mix (Figures 3F–3H). Consistent with a role of Notch in 2° fate induction, we observed that the first errors to increasing Notch signaling uniformly in the Pn.p cells were induction of 2° fate for P3.p, P4.p, or P8.p (line JU2064, Figures 3F and 3G for

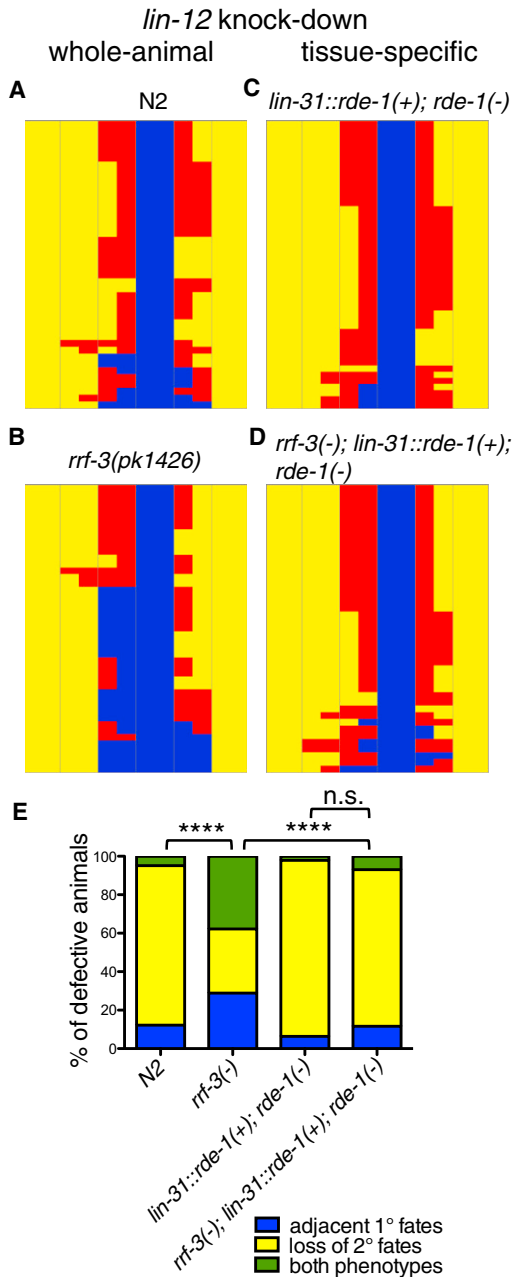


Figure 4. The Role of Notch in the Pn.p Cells Is Mostly to Promote the 2° Fate

(A–D) Phenotypic scoring of Pn.p fates of defective animals upon *lin-12* RNAi of N2, $n = 42$ (A), *rrf-3(pk1426)*, $n = 45$ (B), *lin-31::rde-1(+); rde-1(ne219)*, $n = 46$ (C), and *rrf-3(pk1426); lin-31::rde-1(+); rde-1(ne219)*, $n = 43$ (D) animals. The transgene-mediated rescue of RNAi competence is not fully penetrant, and the wild-type animals are not presented for simplicity.

(E) Quantification of the RNAi phenotypes divided in three classes: adjacent 1° fates (blue), loss of 2° fates (yellow), and both phenotypes in the same individual (green). Differences in the frequency of these classes between N2 and *rrf-3(pk1426)* or *rrf-3(pk1426)* and *rrf-3(pk1426); lin-31::rde-1(+); rde-1(ne219)* animals are significant with a chi-square test ($p < 0.0001$).

7% penetrant vulval defects). Higher Notch overexpression resulted in all Pn.p cells but P6.p adopting the 2° fate (line JU2060, Figure 3H for 100% penetrant vulval defects).

Therefore, our tissue-specific Notch perturbations highlight loss or gain of 2° fates as the first responses to variation in pathway dose, in contrast to the results previously obtained using *lin-12* mutant alleles (Figures 3E and 3I) (Sternberg and Horvitz, 1989; Sundaram and Greenwald, 1993). We conclude that the vulval patterning phenotypes of *lin-12* mutants are dictated by the changes in anchor cell specification (Figure 3I).

Quantitative Interactions between the EGF and Notch Perturbation Lines

We then sought out to investigate nonadditive interactions between perturbations in EGF and Notch pathways by combining their respective dosage perturbation lines with each other. We hypothesized that such a quantitative network analysis can potentially reveal interactions that may have been missed out from classical vulva genetics. Indeed, by assaying multiple combinations (Table S2), we were able to uncover two interesting interactions.

First, we found that the cell fate pattern phenotype of tissue-specific *lin-12* downregulation is modified qualitatively by the addition of a single *lin-3* MosSCI copy (*mfSi3*). This extra *lin-3* copy increases the average *lin-3* mRNA number in the anchor cell by 30% and does not alter the vulval fate pattern (Figure 2). As described above (Figure 3), tissue-specific *lin-12* RNAi results in a frequent transformation of 2° to 3° fate for P5.p and P7.p. The combination of the extra *lin-3* copy with tissue-specific *lin-12* RNAi instead results in a synthetic phenotype, the frequent transformation of 2° to 1° fate for P5.p and P7.p (Figure 5A). This synthetic interaction could also be observed at very low, almost aphenotypic, doses of *lin-12* RNAi (Figure S4A). Therefore, although the major role of LIN-12 in P5.p and P7.p is to promote the 2° fate under wild-type conditions, the inhibition of 1° fate becomes important in situations where *lin-3* expression is even mildly increased (Figure 5B).

To consolidate this finding using stable mutants instead of RNAi, we used a mutation in the Notch coactivator *osm-11*, which has been proposed to facilitate Notch signaling in the Pn.p cells, but not in the anchor cell (Komatsu et al., 2008). Consistent with this role, the *osm-11(rt142)* mutation, which deletes the whole mature protein, phenocopies the tissue-specific *lin-12* knockdown by displaying loss of 2° fates for P5.p and/or P7.p (Figure S4B; Table S2). In the *osm-11(rt142)* mutant background, we observed that two extra copies of *lin-3*, which are normally aphenotypic, can similarly result in the adjacent 1° fate phenotype (Figure S4B). However, it is mostly P7.p in this case that acquires the 1° fate and not P5.p, consistent with the bias of *osm-11* mutants to lose the 2° fate more often in P7.p than P5.p (Figure S4B; Table S2). The genetic interaction between *osm-11(rt142)* and the two extra copies of *lin-3* was also apparent at the level of mean induction index (Figure S4C) and average number of vulval invaginations (Figure S4D).

Second, through our network analysis, we obtained evidence for a synergistic interaction between EGF and Notch in P6.p induction. EGF and Notch are supposed to act antagonistically within a given vulval precursor cell, where both pathways mutually inhibit each other (Berset et al., 2001; Shaye and Greenwald, 2002; Yoo et al., 2004). However, these two pathways may also act synergistically on 2° fate specification, as EGF at low dose

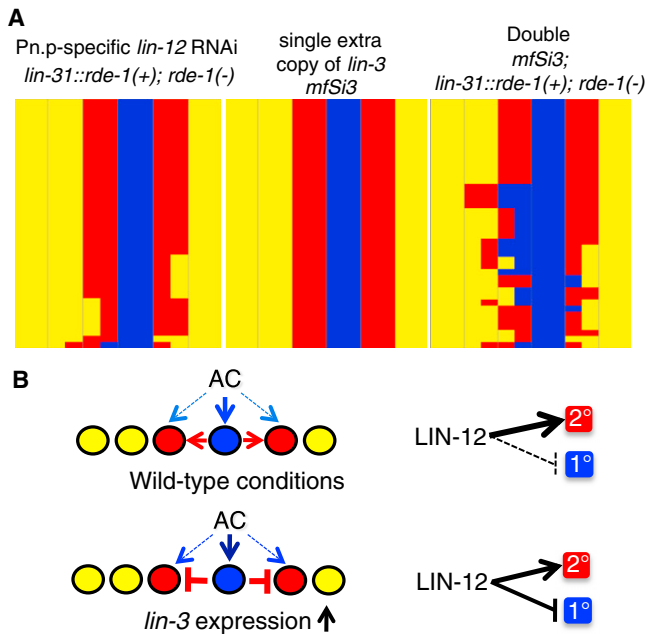


Figure 5. Lateral Inhibition Is Relevant When *lin-3* Dose Is Mildly Increased

(A) Comparison of phenotypic effects on P3.p–P8.p fates of Pn.p-specific *lin-12* RNAi performed in parallel in strains without and with a single extra copy of *lin-3* (*mfSi3*). Note the increased frequency of animals with adjacent 1° fates in the combined treatment (n = 43), a phenotype that is very rare in *lin-31::rde-1(+); rde-1(-)* animals (n = 41) and never observed in animals carrying only the *mfSi3* insertion (n = 100).

(B) Cartoon of our model depicting that the inhibition of 1° fate by LIN-12 is biologically relevant in situations where *lin-3* expression is mildly increased. See also Figure S4 and Table S2.

can promote 2° fate induction (Katz et al., 1995), although it is yet unclear whether this is mediated by Notch signaling. Surprisingly, we found that EGF and Notch can also act synergistically on 1° fate specification, since the P6.p induction defects (1° to 3° fate transformation) conferred by the *lin-3(e1417)* mutation were enhanced by the weak *lin-12(e2621)* mutation (Figure 6A). Because this interaction could be explained by an effect of *lin-12(e2621)* on EGF production from the anchor cell, we also used our *mfSi3[lin-31::lin-12(intra)]* transgene that increases Notch signaling specifically in the Pn.p cells. We observed that the P6.p induction defects of *lin-3(e1417)* (Figure 6A) or *lin-3* RNAi-treated animals (Figure S4E) were partially suppressed, indicating that the Notch-mediated effect on 1° fate is likely confined to Pn.p cells.

A way to interpret this interaction is that the Notch pathway at low dose may be sufficient to promote the 1° fate independently of the anchor cell. We tested this hypothesis by ablating the gonad in a strain carrying the *mfSi3[lin-31::lin-12(intra)]* transgene and the 1° fate marker *egl-17::CFP*. Contrary to the hypothesis, we never observed gonad-independent induction (n = 20). *egl-17::CFP* expression at the P6.px stage (after one division of Pn.p cells) was decreased, consistent with an antagonistic relationship between the two pathways in these conditions (Figure S4F).

We then hypothesized that the synergistic effect of the Notch pathway on 1° fate induction and *egl-17::CFP* expression only

occurs when LIN-3 activity is impaired, as in *lin-3(e1417)* mutants. In the *lin-3(e1417)* background, *egl-17* expression was hardly detectable in Pn.p cells because of low MAPK signaling, but became detectable at the Pn.pxx stage (after the second division round). At this stage, the *lin-31::lin-12(intra)* transgene did not affect the *egl-17::CFP* level in P6.p (Figure S4G), yet resulted in ectopic *egl-17::CFP* expression in other Pn.p cells (9/22 animals), usually P5.p and P7.p, albeit at low levels (Figures 6B–6D and S4H). This ectopic expression was never observed in *lin-3(e1417)* animals without the transgene (n = 15) and rarely with the transgene alone (0/24 animals at Pn.px stage and 1/15 animals at Pn.pxx). Therefore, low hyperactivation of the Notch pathway in a *lin-3* reduction-of-function mutant background can trigger the ectopic expression of a 1° fate marker. We conclude that EGF and Notch can also act in a synergistic way within a cell, perhaps depending on their relative dose, when the EGF pathway is weak.

A Phase Diagram for Vulval Fates in Signaling Pathway Space

To collectively represent the results of our quantitative network analysis, we draw the analogy to a phase diagram. These diagrams present all discrete phases of a system and their occurrence upon quantitative change of parameters, usually physical parameters, such as temperature or pressure. By analogy, such a phase diagram represents here the quantitative state of the vulval cell fate output when the two major signaling pathways are varied genetically (Figure 7).

In Figure 7, the most frequent error patterns are depicted as a function of EGF and Notch pathway activities. In most cases, several cell fate pattern states can coexist for a given combination of perturbations, due to stochastic variation in the isogenic population. The two axes of the graph are not independent. For example, given that production of the Notch ligands is directly downstream of the EGF pathway, perturbations of *lin-3* expression can have an effect on the lateral signal. However, the reverse is not true: as expected, we observed by smFISH that our tissue-specific Notch perturbations do not change *lin-3* expression in the anchor cell (data not shown).

The robustness of the wild-type pattern to stochastic variation among individuals is gradually lost as the system accumulates quantitative changes in EGF and Notch pathways. As mentioned above, even a combination of aphenotypic perturbations in both pathways can fall out of the robustness zone (mild EGF increase in concert with mild Notch decrease). Similar diagrams of cell fate of single Pn.p cells upon quantitative perturbations indicated that P6.p is more robust than other Pn.p cells for the combinations of perturbations that we assayed (Figure S5A).

Moreover, the induction index does not necessarily vary monotonously along horizontal or vertical lines, that is, when either EGF or Notch activity is varied (Figure 7). For example, in the presence of one extra copy of *lin-3/egl* in the genome, the vulval induction index first decreases and then increases when Notch activity is gradually increased, with a corresponding transition in the vulval fate pattern (Figure S5B).

Previous two-dimensional representations of vulval cell fate as a function of EGF and Notch pathways were distinct, as they represented the theoretical relationship between pathway activities

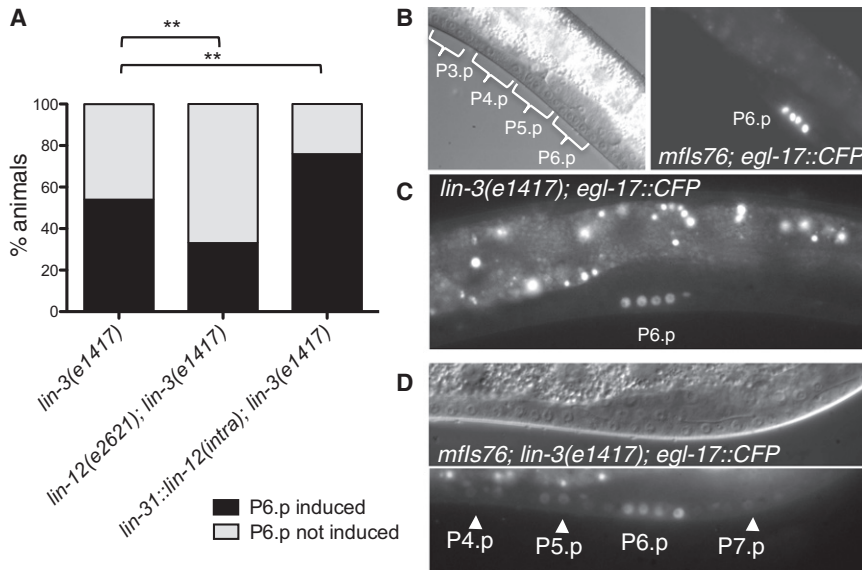


Figure 6. EGF and Notch Can Act in a Synergistic Way within the Pn.p Cells

(A) Graph showing percentage of P6.p induction in double mutant combinations of *lin-3(e1417)* with either *lin-12(e2621)* or *lin-31::lin-12(intra)* (*mfls76*). P6.p induction is 100% for *lin-12(e2621)* and *mfls76* animals. Differences are significant by a Fisher's exact test ($p = 0.0018$ and $p = 0.0039$, respectively).

(B and C) Expression of *egl-17::CFP* is confined to P6.p descendants at the Pn.pxx stage of *mfls76* (B) and *lin-3(e1417)* (C) animals. The left panel in (B) is DIC (note P3.p induction), and the right panel is the cyan fluorescent protein (CFP) signal.

(D) Ectopic *egl-17::CFP* expression in other Pn.p cells is observed in *mfls76; lin-3(e1417)* at the Pn.pxx stage. White arrowheads point to weak ectopic expression in P4.p, P5.p, and P7.p. The upper panel is DIC, and the lower panel is CFP channel.

See also Figure S4 and Table S2.

in a given cell (i.e., variables, not parameters in the model) and its cell fate (Giurumescu et al., 2006, 2009; Hoyos et al., 2011). Instead, what we represent here is the relationship between some upstream parameters, such as *lin-3/egf* synthesis rate and *lin-12/Notch* synthesis and activation rate, which we could experimentally control, and the fates of all six cells.

DISCUSSION

Here we performed a quantitative analysis of an intercellular signaling network by modulating each signaling pathway in a tissue-specific manner. This study significantly improves our quantitative understanding of the system and its underlying patterning mechanisms.

Robustness of the Vulval Cell Fate Pattern to *lin-3* Dose

First, we demonstrated that genetic variation in *lin-3/egf* expression can be buffered by the system between an average number of 15 and 50 *lin-3* mRNA molecules at the time of induction. With an average of 27 *lin-3* mRNA molecules, the wild-type reference strain is located midway, at a 2-fold distance of either boundary. Given the high reproducibility of the *C. elegans* vulval cell fate pattern in different environments or genetic backgrounds (Félix, 2007; Kiontke et al., 2007; Braendle and Félix, 2008), this finding raises the question of whether the lack of errors reflects lack of *lin-3* expression variation outside this buffering zone. It will be important to test this hypothesis by quantitative analysis of *lin-3* transcription in different growth conditions or in *C. elegans* isolates other than N2. One possibility is that *lin-3* transcription is tightly regulated so that variation is low, and another is that such variation is present, but effectively buffered downstream in the system.

What is the mechanistic basis for the robustness of wild-type patterning to *lin-3* dose? We suggest that the buffering of variation in *lin-3* expression by the system simply stems from the spatial cellular context (the row of cells with P6.p being the closest to the anchor cell) and the network topology (induction by EGF of the 1° fate in P6.p and of 2° fate by lateral induction

in its neighbors), without the need to invoke robustness-conferring genes or mechanisms (Félix and Barkoulas, 2012). By finely varying *lin-3* dose, we defined the first-appearing cell fate pattern errors and thereby reveal the corresponding defective mechanisms that allow and limit this robustness.

When mean *lin-3* level is lowered, two types of error appear concomitantly: (1) a 2° to 3° fate transformation, generally in the outer daughters of P5.p and P7.p and (2) a loss of all induced cell fates. Thus, the lowest activation level of the Ras pathway allowing for 1° fate activation in P6.p also generally activates the 2° fate in its neighbors—yet the signal is not always sufficient in the outer daughter of P5.p/P7.p. In sum, normal patterning requires a simple threshold of Ras-MAPK pathway activation in P6.p: wild-type cell fates can then be patterned by MAPK-mediated activation of the 1° fate in P6.p and lateral induction of 2° fates.

When mean *lin-3* level is elevated, the limit compatible with wild-type patterning stems from the fact that EGF can act as a long-range secreted signal. Intermediate EGF levels experienced by P5.p and P7.p are permissible as they activate the 2° fate. Higher *egf* doses may theoretically cause direct ectopic induction of P4.p/P8.p or transform P5.p/P7.p to the 1° fate (Giurumescu et al., 2009; Hoyos et al., 2011). We found that, upon *lin-3* overexpression, the first-appearing defect is the occurrence of adjacent 1° fates, with ectopic induction of a 2° fate next to the additional 1° fate (Figure 1). Thus, at high *egf* levels, lateral inhibition of P5.p/P7.p is the limiting mechanism. However, the loss of 2° fates upon tissue-specific downregulation of LIN-12 indicates that lateral inhibition is not essential under normal conditions, perhaps because the amount of EGF reaching P5.p/P7.p is not sufficient for them to adopt the 1° fate.

We note that a similar first deviant pattern to *lin-3* overexpression had previously been observed in *C. briggsae* (Félix, 2007), but appears contradictory to a recent experiment in *C. elegans*, where P4.p was induced in the absence of P5.p fate transformation to the 1° fate (Hoyos et al., 2011). We explain this discrepancy by the fact that the previous result was based on overexpression of the *lin-3(e1417)* sequence, which is defective

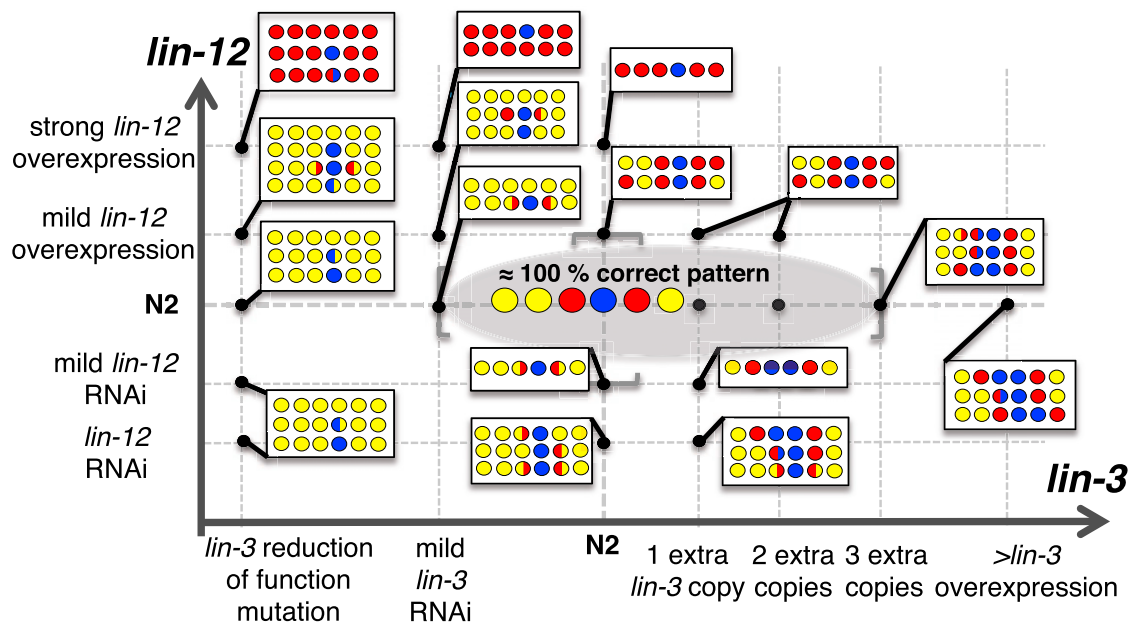


Figure 7. A Vulval Fate Map

Cartoon depicting the most representative vulval fate pattern variants observed upon quantitative perturbation of the EGF and Notch pathways. Within each rectangle, the fate patterns are presented in decreasing order of frequency from top to bottom. Notch perturbations are tissue-specific for the Pn.p cells, and *lin-3* dosage perturbations affect *lin-3* transcription in the anchor cell. Strong *lin-12* overexpression refers to *mfls72*, mild *lin-12* overexpression to *mfls76*, *lin-3* reduction of function to *lin-3(e1417)*, one extra *lin-3* copy to *mfSi3* or *mfSi1*, two extra copies to *mfSi2* or *mfSi1*; *mfSi3*, three extra copies to *mfSi1*; *mfSi2*, and stronger (>) *lin-3* overexpression to *mfls54* or *mfls55*. In most cases, the frequencies of these errors are low, as the majority of the animals retain the wild-type fate pattern (with the exception of lines carrying the *mfls72* transgene, where errors are highly penetrant).

See also Figure S5 and Table S2.

for anchor cell expression and thus likely produced a less localized signal. Consistent with this, induction of P4.p before the occurrence of adjacent 1° fates is also observed in backgrounds that harbor multivulva mutations, such as *lin-15* or *let-60(gf)* (Sternberg, 1988, 2005; Sternberg and Horvitz, 1989; Han et al., 1990; Sternberg and Han, 1998; Félix, 2012) or upon heat-shock-mediated overexpression of *lin-3* (Katz et al., 1995). In all cases, the treatment results in either ectopic *lin-3* overexpression (Saffer et al., 2011) or general ligand-independent gain-of-activity in the Ras-MAKP kinase pathway rather than an increase in *lin-3* expression within the anchor cell.

Role of LIN-12/Notch Activity in Vulval Precursor Cells

Second, we re-evaluated the role of the Notch pathway in vulval precursor cells using tissue-specific modulations of its activity. This approach proved informative, since we observed dramatically different cell fate pattern phenotypes upon tissue-specific alteration compared to those of *lin-12* mutants (Figure 3I). We find that the main role of the Notch pathway in vulval precursor cells is to induce the 2° fate, but that the system is poised close to the threshold where the Notch pathway’s role transitions from induction to inhibition. These findings are in keeping with a previous report that broad downregulation of the Notch ligands leads in the wild-type to some loss of 2° fates, but in a sensitized background showing ectopic *lin-3* expression to an increased frequency of adjacent 1° fates (Chen and Greenwald, 2004).

These results challenge some textbook depictions of wild-type vulval development where Notch acts as a lateral inhibitory

signal (for example, see Griffiths et al., 2000). Note, however, that the major role of Notch in lateral induction rather than inhibition does not contradict nor eliminate the fact that EGF is able to reach other cells than P6.p in a graded manner. Importantly, both our *lin-3* dose-response curve and the switch in mode of action of the Notch pathway are quantitative results, thus can be readily used to challenge the existing mathematical models of vulval cell fate patterning (Giurumescu et al., 2006; Hoyos et al., 2011).

Epistatic Interactions between EGF and Notch Pathways

We conducted a quantitative network analysis by combining dosage-perturbations in the two pathways and investigating their cumulative effect. Even for a system like the *C. elegans* vulva, where the genetics have been exhaustively carried out, we did observe unexpected interactions, highlighting the significance of the approach. For example, we found that a single extra copy of *lin-3* can switch the Pn.p-specific function of Notch from lateral induction to lateral inhibition. This system feature had previously been missed, partly because of the lack of tissue-specific Notch perturbations and partly due to the absence of mild, aphenotypic EGF dosage-perturbations. Importantly, this finding may have some evolutionary implications, as the distinction between lateral inhibition and induction for Notch relies on silent variation in EGF pathway levels. Through analysis of EGF/Ras pathway activity reporter expression in different *C. elegans* isolates, we have previously revealed such silent (cryptic) variation (Milloz et al., 2008). Therefore, the

relative mode of action of the Notch pathway in the Pn.p cells may evolve, concomitant with variation in EGF pathway activity.

Another surprising result concerns the synergistic interaction between EGF and Notch pathways in 1° fate induction of P6.p at low LIN-3 levels. This interaction suggests that another layer of robustness may be provided by Notch activating the 1° fate in situations where LIN-3 activity is partially impaired. Although the mechanistic basis of this interaction remains unclear, studies in *Drosophila* have identified both positive and negative components of the EGF pathway as direct Notch targets, illustrating that Notch activation can lead to opposing effects on EGF signaling, even within the same developmental context (Krejci et al., 2009). Consistent with this genetic interaction, we found ectopic expression of the 1° fate marker *egl-17::CFP* in the Pn.p cells of *lin-31::lin-12(intra); lin-3(e1417)* animals. In addition, previous studies have identified a link between the vulval precursor cell cycle and the temporal window of their competence and commitment to a particular cell fate (Ambros, 1999; Wang and Sternberg, 1999), indicating that the effects of these pathways along the cell cycle may underlie some of the interactions observed in phase space. Specifically, Notch signaling has been proposed to maintain competence and thus prolong the developmental window in which Pn.p cells can respond to morphogenetic signals, such as LIN-3 (Wang and Sternberg, 1999). This phenomenon could explain the partial rescue of P6.p induction defects of *lin-3(e1417)* animals in the presence of a *lin-31::lin-12(intra)* transgene. It is notable that nonintuitive interactions in sensitized backgrounds, including this very one, were also anticipated by a recent geometric model of vulval cell specification (Corson and Siggia, 2012), where a signal that pushes a cell in one direction can displace cell fate outcomes in different directions as a result of nonlinear dynamic flow in the landscape defined by the model.

More broadly, our network analysis highlights important considerations when interpreting genetic results. In this system, effects on the induction index or the average number of vulval invaginations have been repeatedly used to address the function of newly identified regulators. Intuitively, factors found to increase the induction index or the number of pseudovulvae of a given background are believed to typify positive vulval regulators. However, we demonstrated that, depending on the relative dose of the EGF and Notch pathways, the same pathway can increase the induction index both when its activity increases and decreases. For example, in the presence of an extra copy of *lin-3* in the genome, both an increase and decrease of Notch activity in the Pn.p cells will increase the induction index (Figure S5B). In this case, when Notch activity is reduced, P5.p acquires the 1° fate and promotes the induction of P4.p by secreting Notch ligands; when Notch activity is increased, additional cells adopt a 2° fate. The distinction thus becomes clear when the cell fate pattern, and not only the induction index, is taken into account. Another complication is that we occasionally observed the same fate patterns upon Notch or EGF dosage perturbations. For example, loss of 2° fates for P5.p and P7.p can be observed with either mild decrease of EGF or Notch and adjacent 1° fates for P5.p and P6.p with either strong increase of EGF or mild increase of EGF together with a decrease in Notch. This illustrates that the definition of a positive or negative vulval regulator and its assignment to a particular signaling

pathway can be ambiguous, unless precise scorings of actual vulval fates are performed and quantitative context-dependent aspects of interactions in the network are considered.

Within the *Caenorhabditis* genus, the vulval cell fate pattern is morphologically invariant, yet it evolves by accumulating cryptic variation (Félix, 2007; Milloz et al., 2008). Some of this variation may concern quantitative evolution in the strength of EGF inductive and Notch lateral signaling pathways. To this end, comparisons with the behavior of the *C. elegans* vulva upon quantitative pathway change will likely give insights into the evolution of this system.

EXPERIMENTAL PROCEDURES

lin-3 Overexpression Strains and Genetics

lin-3 overexpression lines were created by amplifying a 5.2 kb genomic fragment, as described in Hoyos et al. (2011). Extrachromosomal arrays were integrated by γ -ray irradiation and then backcrossed four times to N2. To create the *lin-3* insertions by MosSCI, the same 5.2 kb fragment was amplified using primers *lin-3AvrII* and *lin-3XhoI* and then cloned into pCFJ151 (chromosome II targeting vector) and pCFJ178 (chr. IV) (Frøkjær-Jensen et al., 2008) as an *AvrII/XhoI* fragment. Injections and recovery of insertions was performed using the direct insertion protocol (Frøkjær-Jensen et al., 2008). Insertions were verified by PCR using primers flanking the insertion site, and copy number was tested by pyrosequencing (see Supplemental Experimental Procedures).

lin-3(e1417)+ heterozygotes were obtained by crossing *lin-3(e1417)* mutants carrying a linked *myo2::GFP* insertion with a strain (BJ49) carrying an *ifb-2::CFP* insertion on chromosome IV and selecting animals expressing both reporters.

lin-12 Dosage Alteration

The *lin-31::lin-12(intraΔP)::unc-54* construct was built as described in Li and Greenwald (2010) by amplifying the intracellular domain of *lin-12* from genomic DNA using primers *lin-12intraBglII* and *lin-12intraNotI* and then cloning the product into pB253 (Tan et al., 1998) as a *BglII/NotI* fragment. We injected this construct at two final concentrations in the injection mix: 20 ng/ μ l to obtain mild overexpression lines (JU2064) and 75 ng/ μ l for strong overexpression lines (JU2060). Extrachromosomal arrays were integrated by γ -ray irradiation and backcrossed five to seven times to N2.

To create the *lin-31::rde-1(+):unc-54* rescuing construct, the full *rde-1* coding sequence was amplified from genomic N2 DNA using primers *rde-1F1* and *rde-1R1* and then cloned into pGEM-T-easy (Promega). The *rde-1* open reading frame was transferred from pGEM-T-easy to pB253 as a *NotI* fragment. Insert direction and sequence fidelity were verified by sequencing. *mfls70* represents a spontaneous integration event of this transgene into chromosome IV.

Microscopy and Phenotypic Characterization

To score vulval cell fates, animals were analyzed at the L4 stage by differential interference contrast (DIC) microscopy, using a 100 \times lens. Standard criteria were used to assign fates (Katz et al., 1995; Félix, 2007), such as the final number cells for each lineage, their relative position around the vulva, and whether they are attached to the cuticle. See also Supplemental Experimental Procedures.

Single Molecule Fluorescence In Situ Hybridization

Synchronized populations of L3 stage animals were prepared by bleaching adults to recover their embryos. These embryos were washed with M9 and plated on standard nematode growth medium plates, allowing them to hatch and grow at 20° for 32–35 hr before fixation. smFISH was performed as described before (Raj et al., 2008), using custom-made probes labeled with Cy5 for *lin-3* and Alexa-594 for *lag-2*. The oligonucleotide sequences used for each probe can be found in the Supplemental Experimental Procedures. From each animal, we acquired a Z-stack of 30 sections, using a Nikon Ti-e inverted microscope or an upright Zeiss AxioImager M1, both equipped with a Pixis 1024B camera (Princeton Instruments) and a Lumen 200 metal arc

lamp (Prior Scientific). Quantification of spots was performed as described (Raj et al., 2008), using a custom-made routine on Matlab, optimized for anchor cell measurements. To minimize variation due to developmental stage, only animals with gonad length >350 pixels (43.75 μm) were included in the quantification. Quantification was not performed in strong *lin-3* overexpression lines, such as *syls1* (PS1123), because the *lin-3* signal in the anchor cell could not be resolved into individual fluorescent spots. Statistical comparisons were performed using R and Graphpad Prism 5.

SUPPLEMENTAL INFORMATION

Supplemental Information includes five figures, two tables, and Supplemental Experimental Procedures and can be found with this article online at <http://dx.doi.org/10.1016/j.devcel.2012.12.001>.

ACKNOWLEDGEMENTS

We thank Christian Braendle for critical reading of the manuscript. This work was funded by grants from the Association pour la Recherche sur le Cancer (#1044) and the Agence Nationale de la Recherche (08 BLAN-0024) to M.-A.F. We also acknowledge the support of the Bettencourt Foundation for a Coup d'Élan (to M.-A.F.), EMBO for a short-term fellowship (to M.B.), and Human Frontiers Science Program (to J.S.v.Z.). During the course of this work, M.-A.F. was first a principal investigator at CNRS and is now a professor at Ecole Normale Supérieure.

Received: August 8, 2012

Revised: November 12, 2012

Accepted: December 3, 2012

Published: January 14, 2013

REFERENCES

- Ambros, V. (1999). Cell cycle-dependent sequencing of cell fate decisions in *Caenorhabditis elegans* vulva precursor cells. *Development* 126, 1947–1956.
- Ansel, J., Bottin, H., Rodriguez-Beltran, C., Damon, C., Nagarajan, M., Fehrmann, S., François, J., and Yvert, G. (2008). Cell-to-cell stochastic variation in gene expression is a complex genetic trait. *PLoS Genet.* 4, e1000049.
- Barkai, N., and Leibler, S. (1997). Robustness in simple biochemical networks. *Nature* 387, 913–917.
- Berset, T., Hoier, E.F., Battu, G., Canevascini, S., and Hajnal, A. (2001). Notch inhibition of RAS signaling through MAP kinase phosphatase LIP-1 during *C. elegans* vulval development. *Science* 291, 1055–1058.
- Braendle, C., and Félix, M.-A. (2008). Plasticity and errors of a robust developmental system in different environments. *Dev. Cell* 15, 714–724.
- Chen, N., and Greenwald, I. (2004). The lateral signal for LIN-12/Notch in *C. elegans* vulval development comprises redundant secreted and transmembrane DSL proteins. *Dev. Cell* 6, 183–192.
- Corson, F., and Siggia, E.D. (2012). Geometry, epistasis, and developmental patterning. *Proc. Natl. Acad. Sci. USA* 109, 5568–5575.
- Csete, M.E., and Doyle, J.C. (2002). Reverse engineering of biological complexity. *Science* 295, 1664–1669.
- Eldar, A., Dorfman, R., Weiss, D., Ashe, H., Shilo, B.Z., and Barkai, N. (2002). Robustness of the BMP morphogen gradient in *Drosophila* embryonic patterning. *Nature* 419, 304–308.
- Félix, M.-A. (2007). Cryptic quantitative evolution of the vulva intercellular signaling network in *Caenorhabditis*. *Curr. Biol.* 17, 103–114.
- Félix, M.A. (2012). *Caenorhabditis elegans* vulval cell fate patterning. *Phys. Biol.* 9, 045001.
- Félix, M.A., and Barkoulas, M. (2012). Robustness and flexibility in nematode vulva development. *Trends Genet.* 28, 185–195.
- Ferguson, E.L., and Horvitz, H.R. (1985). Identification and characterization of 22 genes that affect the vulval cell lineages of the nematode *Caenorhabditis elegans*. *Genetics* 110, 17–72.
- Ferguson, E.L., Sternberg, P.W., and Horvitz, H.R. (1987). A genetic pathway for the specification of the vulval cell lineages of *Caenorhabditis elegans*. *Nature* 326, 259–267.
- Frøkjær-Jensen, C., Davis, M.W., Hopkins, C.E., Newman, B.J., Thummel, J.M., Olesen, S.P., Grunnet, M., and Jørgensen, E.M. (2008). Single-copy insertion of transgenes in *Caenorhabditis elegans*. *Nat. Genet.* 40, 1375–1383.
- Giurumescu, C.A., Sternberg, P.W., and Asthagiri, A.R. (2006). Intercellular coupling amplifies fate segregation during *Caenorhabditis elegans* vulval development. *Proc. Natl. Acad. Sci. USA* 103, 1331–1336.
- Giurumescu, C.A., Sternberg, P.W., and Asthagiri, A.R. (2009). Predicting phenotypic diversity and the underlying quantitative molecular transitions. *PLoS Comput. Biol.* 5, e1000354.
- Greenwald, I.S., Sternberg, P.W., and Horvitz, H.R. (1983). The *lin-12* locus specifies cell fates in *Caenorhabditis elegans*. *Cell* 34, 435–444.
- Gregor, T., Wieschaus, E.F., McGregor, A.P., Bialek, W., and Tank, D.W. (2007). Stability and nuclear dynamics of the bicoid morphogen gradient. *Cell* 130, 141–152.
- Griffiths, A., Miller, J., Suzuki, D., Lewontin, R., and Gelbart, W. (2000). *An Introduction to Genetic Analysis*, Seventh Edition (New York: W.H. Freeman).
- Gutiérrez, J. (2009). A developmental systems perspective on epistasis: computational exploration of mutational interactions in model developmental regulatory networks. *PLoS ONE* 4, e6823.
- Han, M., Aroian, R.V., and Sternberg, P.W. (1990). The let-60 locus controls the switch between vulval and nonvulval cell fates in *Caenorhabditis elegans*. *Genetics* 126, 899–913.
- Hill, R.J., and Sternberg, P.W. (1992). The gene *lin-3* encodes an inductive signal for vulval development in *C. elegans*. *Nature* 358, 470–476.
- Hoyos, E., Kim, K., Milloz, J., Barkoulas, M., Pénigault, J.B., Munro, E., and Félix, M.A. (2011). Quantitative variation in autocrine signaling and pathway crosstalk in the *Caenorhabditis* vulval network. *Curr. Biol.* 21, 527–538.
- Hwang, B.J., and Sternberg, P.W. (2004). A cell-specific enhancer that specifies *lin-3* expression in the *C. elegans* anchor cell for vulval development. *Development* 131, 143–151.
- Katz, W.S., Hill, R.J., Clandinin, T.R., and Sternberg, P.W. (1995). Different levels of the *C. elegans* growth factor LIN-3 promote distinct vulval precursor fates. *Cell* 82, 297–307.
- Kenyon, C. (1995). A perfect vulva every time: gradients and signaling cascades in *C. elegans*. *Cell* 82, 171–174.
- Kiontke, K., Barrière, A., Kolotuev, I., Podbilewicz, B., Sommer, R.J., Fitch, D.H.A., and Félix, M.-A. (2007). Trends, stasis, and drift in the evolution of nematode vulva development. *Curr. Biol.* 17, 1925–1937.
- Kitano, H. (2004). Biological robustness. *Nat. Rev. Genet.* 5, 826–837.
- Kitano, H. (2007). A robustness-based approach to systems-oriented drug design. *Nat. Rev. Drug Discov.* 6, 202–210.
- Komatsu, H., Chao, M.Y., Larkins-Ford, J., Corkins, M.E., Somers, G.A., Tucey, T., Dionne, H.M., White, J.Q., Wani, K., Boxem, M., and Hart, A.C. (2008). OSM-11 facilitates LIN-12 Notch signaling during *Caenorhabditis elegans* vulval development. *PLoS Biol.* 6, e196.
- Krejčí, A., Bernard, F., Housden, B.E., Collins, S., and Bray, S.J. (2009). Direct response to Notch activation: signaling crosstalk and incoherent logic. *Sci. Signal.* 2, ra1.
- Levy, S.F., and Siegal, M.L. (2008). Network hubs buffer environmental variation in *Saccharomyces cerevisiae*. *PLoS Biol.* 6, e264.
- Li, J., and Greenwald, I. (2010). LIN-14 inhibition of LIN-12 contributes to precision and timing of *C. elegans* vulval fate patterning. *Curr. Biol.* 20, 1875–1879.
- Ma, W., Lai, L., Ouyang, Q., and Tang, C. (2006). Robustness and modular design of the *Drosophila* segment polarity network. *Mol. Syst. Biol.* 2, 70.
- Masel, J., and Siegal, M.L. (2009). Robustness: mechanisms and consequences. *Trends Genet.* 25, 395–403.
- Meir, E., von Dassow, G., Munro, E., and Odell, G.M. (2002). Robustness, flexibility, and the role of lateral inhibition in the neurogenic network. *Curr. Biol.* 12, 778–786.

- Milloz, J., Duveau, F., Nuez, I., and Félix, M.-A. (2008). Intraspecific evolution of the intercellular signaling network underlying a robust developmental system. *Genes Dev.* 22, 3064–3075.
- Moriya, H., Shimizu-Yoshida, Y., and Kitano, H. (2006). In vivo robustness analysis of cell division cycle genes in *Saccharomyces cerevisiae*. *PLoS Genet.* 2, e111.
- Pénigault, J.B., and Félix, M.A. (2011). High sensitivity of *C. elegans* vulval precursor cells to the dose of posterior Wnts. *Dev. Biol.* 357, 428–438.
- Phillips, P.C. (2008). Epistasis—the essential role of gene interactions in the structure and evolution of genetic systems. *Nat. Rev. Genet.* 9, 855–867.
- Qadota, H., Inoue, M., Hikita, T., Köppen, M., Hardin, J.D., Amano, M., Moerman, D.G., and Kaibuchi, K. (2007). Establishment of a tissue-specific RNAi system in *C. elegans*. *Gene* 400, 166–173.
- Raj, A., van den Bogaard, P., Rifkin, S.A., van Oudenaarden, A., and Tyagi, S. (2008). Imaging individual mRNA molecules using multiple singly labeled probes. *Nat. Methods* 5, 877–879.
- Raj, A., Rifkin, S.A., Andersen, E., and van Oudenaarden, A. (2010). Variability in gene expression underlies incomplete penetrance. *Nature* 463, 913–918.
- Saffer, A.M., Kim, D.H., van Oudenaarden, A., and Horvitz, H.R. (2011). The *Caenorhabditis elegans* synthetic multivulva genes prevent ras pathway activation by tightly repressing global ectopic expression of *lin-3* EGF. *PLoS Genet.* 7, e1002418.
- Shaye, D.D., and Greenwald, I. (2002). Endocytosis-mediated downregulation of LIN-12/Notch upon Ras activation in *Caenorhabditis elegans*. *Nature* 420, 686–690.
- Siegel, M.L., and Bergman, A. (2002). Waddington's canalization revisited: developmental stability and evolution. *Proc. Natl. Acad. Sci. USA* 99, 10528–10532.
- Simmer, F., Tijsterman, M., Parrish, S., Koushika, S.P., Nonet, M.L., Fire, A., Ahringer, J., and Plasterk, R.H. (2002). Loss of the putative RNA-directed RNA polymerase RRF-3 makes *C. elegans* hypersensitive to RNAi. *Curr. Biol.* 12, 1317–1319.
- Simske, J.S., and Kim, S.K. (1995). Sequential signalling during *Caenorhabditis elegans* vulval induction. *Nature* 375, 142–146.
- Sternberg, P.W. (1988). Lateral inhibition during vulval induction in *Caenorhabditis elegans*. *Nature* 335, 551–554.
- Sternberg, P.W. (2005). Vulval development. In *Wormbook, The C. elegans Research Community*, ed., <http://dx.doi.org/10.1895/wormbook.1.6.1>, www.wormbook.org.
- Sternberg, P.W., and Horvitz, H.R. (1989). The combined action of two intercellular signaling pathways specifies three cell fates during vulval induction in *C. elegans*. *Cell* 58, 679–693.
- Sternberg, P.W., and Han, M. (1998). Genetics of RAS signaling in *C. elegans*. *Trends Genet.* 14, 466–472.
- Struhl, G., Fitzgerald, K., and Greenwald, I. (1993). Intrinsic activity of the *Lin-12* and *Notch* intracellular domains *in vivo*. *Cell* 74, 331–345.
- Sundaram, M., and Greenwald, I. (1993). Genetic and phenotypic studies of hypomorphic *lin-12* mutants in *Caenorhabditis elegans*. *Genetics* 135, 755–763.
- Tan, P.B., Lackner, M.R., and Kim, S.K. (1998). MAP kinase signaling specificity mediated by the LIN-1 Ets/LIN-31 WH transcription factor complex during *C. elegans* vulval induction. *Cell* 93, 569–580.
- von Dassow, G., Meir, E., Munro, E.M., and Odell, G.M. (2000). The segment polarity network is a robust developmental module. *Nature* 406, 188–192.
- Wagner, A. (2005). *Robustness and Evolvability in Living Systems* (Princeton, NJ: Princeton University Press).
- Wang, M., and Sternberg, P.W. (1999). Competence and commitment of *Caenorhabditis elegans* vulval precursor cells. *Dev. Biol.* 212, 12–24.
- Yoo, A.S., Bais, C., and Greenwald, I. (2004). Crosstalk between the EGFR and LIN-12/Notch pathways in *C. elegans* vulval development. *Science* 303, 663–666.
- Zand, T.P., Reiner, D.J., and Der, C.J. (2011). Ras effector switching promotes divergent cell fates in *C. elegans* vulval patterning. *Dev. Cell* 20, 84–96.